ENGPHYS 3BA3

Electronics I: Circuits with Non-Linear and Active Components

The Design Project - The Ultrasonic Range Finder

Ebeze Obianuju

400509852

Angel Zou

400514526

Dr. Adriaan Buijs

Reza Shahzadeh

December 4th 2025

McMaster University

Abstract

This design project served as a final demonstration of the concepts covered throughout the course, bringing them together into one complete system. The goal was to construct an ultrasonic range finder capable of detecting objects between 10cm and 99cm with an accuracy of ±1cm. The circuit was developed using knowledge gained from lectures and labs, along with the ICs and components available in lab. Before building, the system was planned using schematics, timing diagrams, and block-level design. Testing our assembly bit by bit in Multisim, after which the circuit was assembled on a breadboard. By the end of the process, the sensor functioned as intended, demonstrating strong understanding of the material and successful implementation of the design. Performance was verified by measuring the distance to a laptop placed at different positions and checking that the readings on the display. Component values were adjusted when required to improve accuracy. Overall, the project confirmed that the target specifications were achieved, and the ultrasonic range finder operated reliably.

Contents

Introduction

This project involved designing and building an ultrasonic range-finder capable of measuring the distance between a target object and a sensing unit using high-frequency acoustic waves. The device operates by emitting a timed burst of ultrasonic energy, receiving the reflected signal, and converting the measured time-of-flight into a visible distance reading shown on dual seven-segment displays. The expected measurement span was approximately 10 cm to 99 cm, with a resolution goal of ±1 cm, achieved using only discrete ICs, passive components, and breadboard prototyping.

To accomplish this, several key sub-systems were developed and integrated:
- A 40 kHz burst generator to excite the transmitting transducer
- A low-level signal amplification stage for the received echo
- Noise filtering and envelope detection to improve signal clarity
- A comparator and digital counting circuit to translate signal timing into numerical distance
- A display driver to output results to seven-segment LEDs

Completing this build required practical application of theoretical concepts covered throughout the course, including signal processing, time-domain measurement, analog-digital interfacing, and hardware troubleshooting. Beyond demonstrating technical understanding, the project emphasized systematic debugging, hardware design strategy, and component-level problem solving. The final working prototype reflects the cumulative learning of the term and illustrates how individual circuit blocks interact to form a complete sensing system.

Theory

Propagation of Ultrasonic Waves

Ultrasonic range finding is based on the transmission and reception of mechanical pressure waves at frequencies above human hearing (>20 kHz). Ultrasonic sensors can measure distance and detect the presence of an object without making physical contact. They do so by producing and monitoring an ultrasonic echo. Depending on the sensor and object properties, the effective range in air is between a few centimeters up to several meters. The ultrasonic sensor (or transducer) generates and emits ultrasonic pulses that are reflected back towards the sensor by an object that is within the field of view of the sensor.

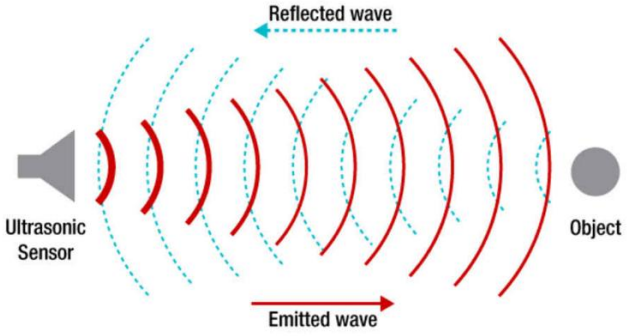

Figure 1: Ultrasonic Time Of Flight Measurement

The ultrasonic sensor is a piezoelectric transducer, which can convert an electrical signal into mechanical vibrations, and mechanical vibrations into an electrical signal. When an alternating voltage is applied at the disc's resonant frequency (≈40 kHz), the crystal lattice expands and contracts rapidly, producing ultrasonic waves.

Likewise, when returning sound waves strike the receiver disc, the mechanical deformation produces a

small AC voltage. This signal is typically in the millivolt range, so it must be amplified and filtered before digital processing.

In a monostatic approach, the ultrasonic sensor is a transceiver which operates as both a speaker and microphone at a single frequency. The sensor can capture the difference in time between the emitted and received echo. Because the speed of sound is a known variable, the captured round-trip time can be used to calculate the distance between the sensor and object. Ultrasonic Distance Calculation is shown below:

$$Distance = \frac{t_{roundtrip} * V_{sound}}{2}$$

The factor of 2 accounts for the wave travelling to the object and back. Accurate distance measurement therefore depends on generating a clean ultrasonic burst and detecting its return clearly above ambient noise. This method of ultrasonic sensing is a time-of-flight measurement based on the propagation time of sound. Note that the speed of sound through air varies by temperature. In dry air at 20°C (68°F), the speed of sound is 343 m/s, or a kilometer in 2.91 s.

Background on Integrated Circuits (ICs)

The ultrasonic range finder constructed in this project relies on a combination of analog and digital integrated circuits (ICs), each responsible for a specific task within the signal generation, conditioning, timing, and display subsystems. Although an exhaustive understanding of semiconductor device physics is not required, a foundational knowledge of IC classifications and their operational characteristics is essential for interpreting system behavior. Two major families of ICs dominate modern electronic design: Complementary Metal-Oxide Semiconductor (CMOS) devices and Transistor–Transistor Logic (TTL) devices.

CMOS ICs are based on complementary pairs of metal-oxide-semiconductor field-effect transistors (MOSFETs), which operate through electric-field-controlled conduction and exhibit extremely low static power consumption, high input impedance, and strong noise immunity [1]. These features make CMOS devices well suited for applications in which small analog signals must propagate through multiple stages without degradation. TTL devices, by contrast, rely on bipolar junction transistors (BJTs) configured in multi-transistor logic networks. BJTs operate via minority carrier injection across two semiconductor junctions, enabling rapid switching at the expense of higher static power consumption [2]. TTL circuits provide predictable logic thresholds and high drive currents, which remain advantageous in timing-sensitive or switching-dominant digital circuits.

For the ultrasonic range finder, the most relevant distinctions between CMOS and TTL technologies involve noise immunity, switching speed, and compatibility with analog inputs. CMOS components, such as the BCD counters and 7-segment drivers used in this project, contribute reduced susceptibility to transient disturbances, which is an important factor because the returned ultrasonic signal is often heavily attenuated and vulnerable to interference. Conversely, TTL-style circuits (and CMOS circuits designed to emulate TTL logic thresholds) support the fast state changes required in timing modules such as the SR latch [3].

ICs Used in the Ultrasonic Range Finder

1. Multivibrators (555 Timer ICs)

A central component of the timing architecture is the 555 timer, a highly flexible IC capable of operating as either an astable or monostable multivibrator [4]. In this project, two standard 555 timers were configured in astable mode:

- One generated the 40 kHz excitation signal required to drive the piezoelectric transmitter.

- The other produced a low-frequency gating waveform (≈2 Hz) to regulate the measurement cycle and enable the ultrasonic burst for only a short duration.

The 555 operates by charging and discharging a timing capacitor between internal comparator thresholds of $\frac{1}{3}V_{CC}$ and $\frac{2}{3}V_{CC}$, making its frequency dependent on external resistor–capacitor (RC) networks. This tunability is essential for aligning the excitation frequency with the resonant frequency of the ultrasonic transducers, thereby maximizing acoustic output efficiency [5].

2. Operational Amplifiers (Op-Amps)

The weak amplitude of the received ultrasonic echo necessitates significant analog amplification before any digital processing can occur. The project uses the LM358P dual operational amplifier, a low-power, low-frequency CMOS op-amp suited for single-supply operation [6]. In a non-inverting configuration, the gain is given by:

$$A_v = 1 + \frac{R_f}{R_{\text{in}}},$$

allowing the designer to precisely control signal magnification while maintaining the phase of the input waveform. Cascading multiple gain stages improves stability, increases bandwidth relative to total gain, and reduces distortion compared to attempting the same gain in a single stage [7]. Because ultrasonic echo amplitudes are typically on the order of several millivolts, this staged approach is necessary to ensure that the comparator receives a signal that crosses the reference threshold reliably.

3. Comparators

Comparators serve as the essential interface between the analog and digital subsystems. Although structurally similar to op-amps, comparators are optimized for fast switching rather than linear amplification. A comparator outputs a digital high or low level depending on whether the input signal exceeds a set reference voltage. When used with a clean reference, comparators function as basic analog-to-digital converters (ADCs) for threshold detection [8]. In this project, the comparator marks the exact moment that the amplified echo surpasses the reference voltage, triggering the “set” input of the SR latch.

Fast comparator response is crucial because timing discrepancies on the order of microseconds can translate directly into centimeter-scale errors in the measured distance. Comparator propagation delay, noise susceptibility, and reference voltage stability therefore affect measurement accuracy.

4. Digital Logic ICs: SR Latch, BCD Counters, and Display Drivers

Several digital ICs coordinate the timing measurement and display:

- SR Latch:
  The Set–Reset latch preserves a digital state representing the interval between the transmitted ultrasonic burst and the detected echo. Resetting occurs at burst emission; setting occurs when the comparator transitions high. This enables the latch output to encode the measured time-of-flight interval [9].
- BCD Counters:
  Binary-Coded Decimal (BCD) counters increment once per clock pulse and roll over after nine counts. By enabling the counter only while the latch output is high, the system effectively converts TOF into a measured count. Cascading counters permits multi-digit measurements and direct numerical readout.
- 7-Segment Display Drivers:

These ICs interpret BCD outputs and activate the corresponding segments of a 7-segment LED display, converting binary-coded values into readable decimal digits. They operate by mapping each binary input pattern to the appropriate LED activation pattern [10].

Together, these digital components form a simple but effective hardware time-to-digital conversion (TDC) system.

Methodology

Planning the Design

Before constructing the circuit, a block and timing diagram was developed to map out the functional sequence of the system. This diagram provided a clear overview of how the transmit burst, amplification stages, comparator output, SR-latch timing, and digital counting interacted. Establishing this visual model early in the design process helped guide the circuit implementation, ensured proper signal flow, and reduced errors during later stages of integration. As we….

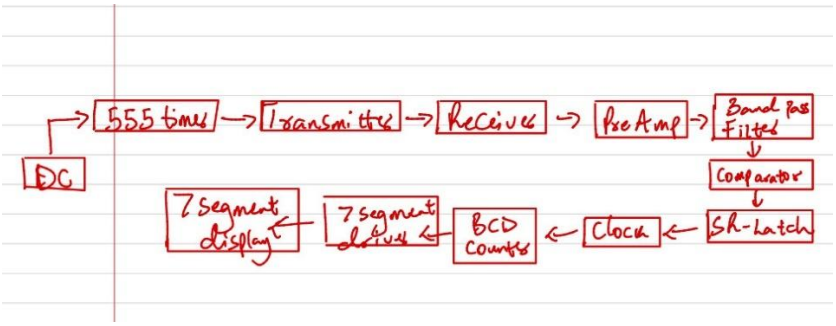

Figure 2: Initial Block Diagram of Circuit

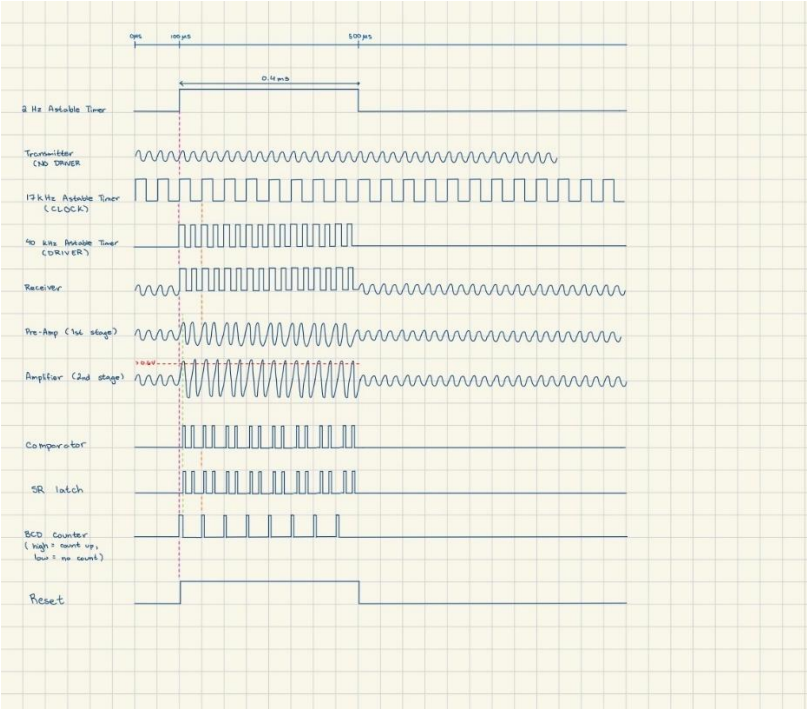

Figure 3: Initial Timing Diagram for Circuit

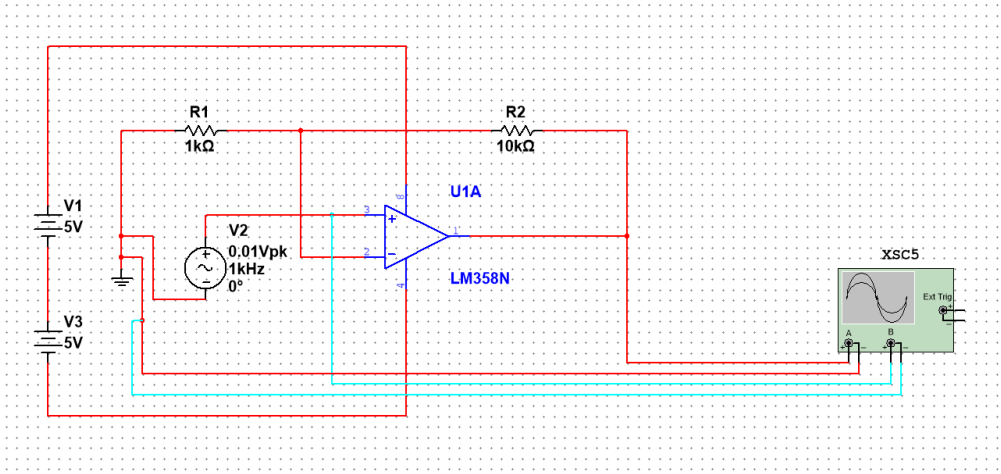

Figure 4: Non-Inverting Amplifier with a gain of 11

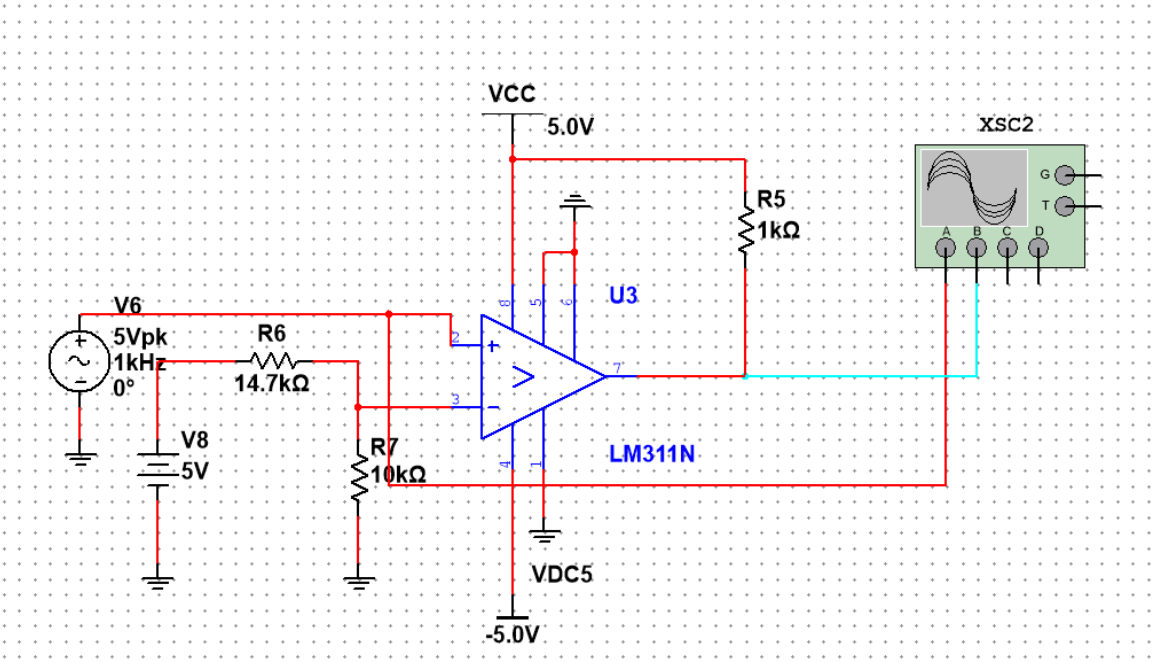

Figure 5: Initial Design of Comparator

Pre-planning the circuit using Multisim simulations, block diagrams, and timing diagrams provided a strong conceptual foundation for how each subsystem was expected to operate and how we would build some of the parts. These tools helped us understand the intended signal flow, timing relationships, and functional dependencies before any hardware was assembled. However, as we began physically building the circuit and connecting components on the breadboard, we identified several practical issues that required adjustments. Component tolerances, noise behavior, and unexpected interactions between stages led us to refine our design in ways that were not immediately apparent during the pre-planning phase.

Constructing the Circuit

The construction of the ultrasonic range finder required the sequential design, testing, and integration of several subsystems: frequency characterization of the transducers, burst generation, signal reception, multi-stage amplification, threshold detection via a comparator, digital pulse latching, and finally distance display through BCD counters and a seven-segment decoder. Each stage was implemented using components available in the laboratory, tested with laboratory equipment, and tuned to achieve the desired timing and gain characteristics.

Characterization of the Ultrasonic Transducer

Before designing the transmit circuitry, my lab partner and I experimentally determined the resonant frequency of the ultrasonic receiver to ensure proper excitation. A function generator was connected directly to the transmitter pins, and a sinusoidal input was swept between 39 kHz and 41 kHz. The corresponding output on the receiver was monitored using a digital oscilloscope. The amplitude response peaked at 40.5 kHz, indicating that this was the effective resonant frequency of the specific transducer used for this experiment. This step is critical because ultrasonic transducers exhibit sharp resonant behavior; driving them at resonance maximizes acoustic output and improves signal-to-noise ratio during reception.

Burst Signal Generation

40.5 kHz Transmit Oscillator

To generate the ultrasonic burst, I constructed an astable multivibrator using a 555 timer IC configured initially for 33 kHz. One of the fixed resistors was replaced by a 100 kΩ potentiometer, allowing fine-tuning of the output frequency. The oscillator was adjusted until the output measured 40.5 kHz on the oscilloscope, matching the transducer resonance for optimal acoustic transmission.

2 Hz Gating Signal

A separate 555-based astable clock was constructed to produce the low-frequency burst trigger. Using

- R1 = 1.470 MΩ,
- R2 = 1.5 kΩ, and
- C = 470 nF,

the resulting timing characteristics were:

- Frequency: 2.08 Hz
- Time High: 479 ms
- Time Low: 0.4 ms

The design intention was to achieve a 0.4 ms high-time, corresponding to the expected round-trip time-of-flight (TOF) for objects within the measurable range. Since the duty cycle produced by the astable was inverted (long high, short low), the signal was passed through a NOT gate, resulting in a clean 0.4 ms high pulse used to trigger the ultrasonic burst.

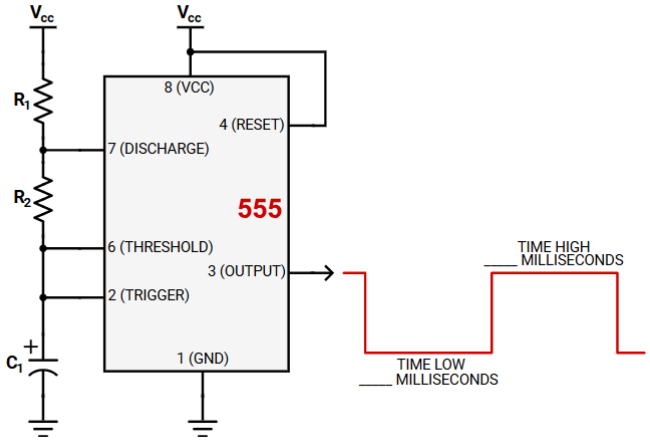

Figure 6: Astable Clock Configuration

Burst Modulation

The output of the 2 Hz gating signal (post-inversion) was fed into Pin 4 (RESET) of the 40.5 kHz oscillator. This gating mechanism ensures that the high-frequency oscillator produces short bursts only during the 0.4 ms interval. The resulting burst waveform was then applied to the TX pin (leftmost terminal) of the transducer.

Signal Reception and Initial Testing

The transmitter and receiver were positioned facing the target. The receiver output was monitored using the oscilloscope while varying the distance and target type (e.g., laptop or cardboard surfaces). This qualitative test ensured that the returning echo produced a measurable waveform before amplification. Once verified, the

RX pin (rightmost terminal) was interfaced with the amplification stage.

Multi-Stage Amplification

The received ultrasonic signal was too weak for direct digital processing; thus, a total gain of approximately 121 was required. To avoid bandwidth limitations and stability issues associated with very high single-stage gains, a two-stage non-inverting amplifier was implemented using LM358P operational amplifiers, each with a gain of 11.

Stage 1 Amplifier

A sinusoidal input from the function generator was used to verify operation prior to connecting the transducer. The gain was set using:

$$A_v = 1 + \frac{R_f}{R_{in}} = 11$$

where resistor values were selected accordingly R_f = 10 kΩ, R_in = 1 kΩ. The output was confirmed to be a clean, non-distorted amplified signal before progressing.

Stage 2 Amplifier

Once Stage 1 was validated, a second LM358P amplifier was constructed with the same gain structure. After confirming its standalone performance, the output of Stage 1 was passed into the input of Stage 2, producing a total gain of approximately 121. The amplified echo signal now had sufficient amplitude for threshold detection.

Comparator Stage

To convert the analog echo signal into a clean digital pulse, a comparator stage was implemented. Based on the design logic from a previous laboratory exercise, the comparator used an LM311P with a reference voltage of 0.6 V, established using a voltage divider.

The comparator output transitions high only when the amplified signal exceeds this reference threshold. This method ensures that only significant echo returns trigger the subsequent digital logic, rather than ambient noise.

SR Latch Design

An SR (Set–Reset) latch was constructed to store the moment when the echo pulse occurred.

- Set (S): Comparator output
- Reset (R): Burst trigger (40.5 kHz timing reference)

The SR latch holds the detection state long enough for the BCD counter to sample it. This design follows the standard SR truth table and ensures proper synchronization between ultrasonic detection and digital counting.

Clocking and Distance Counting

A 17.2 kHz astable 555 oscillator was designed to act as the system clock for the BCD counters. This clock determines how many increments occur during the echo's travel time.

The latch output was connected to the CARRY IN (Pin 5) of the ones-digit BCD counter. The counters were chained such that:

- Ones digit CARRY OUT (Pin 7) → Tens digit CARRY IN (Pin 5)
- Both counters shared a common RESET signal, tied to the low-duty-cycle trigger pulse.

This ensured that each burst initiated a fresh measurement.

Output Display

Finally, the BCD outputs were connected to a seven-segment display decoder using pin assignments from the Digikey datasheets. The decoder drove a two-digit display, corresponding to the measured distance in centimeters based on the number of clock ticks accumulated before the echo was detected.

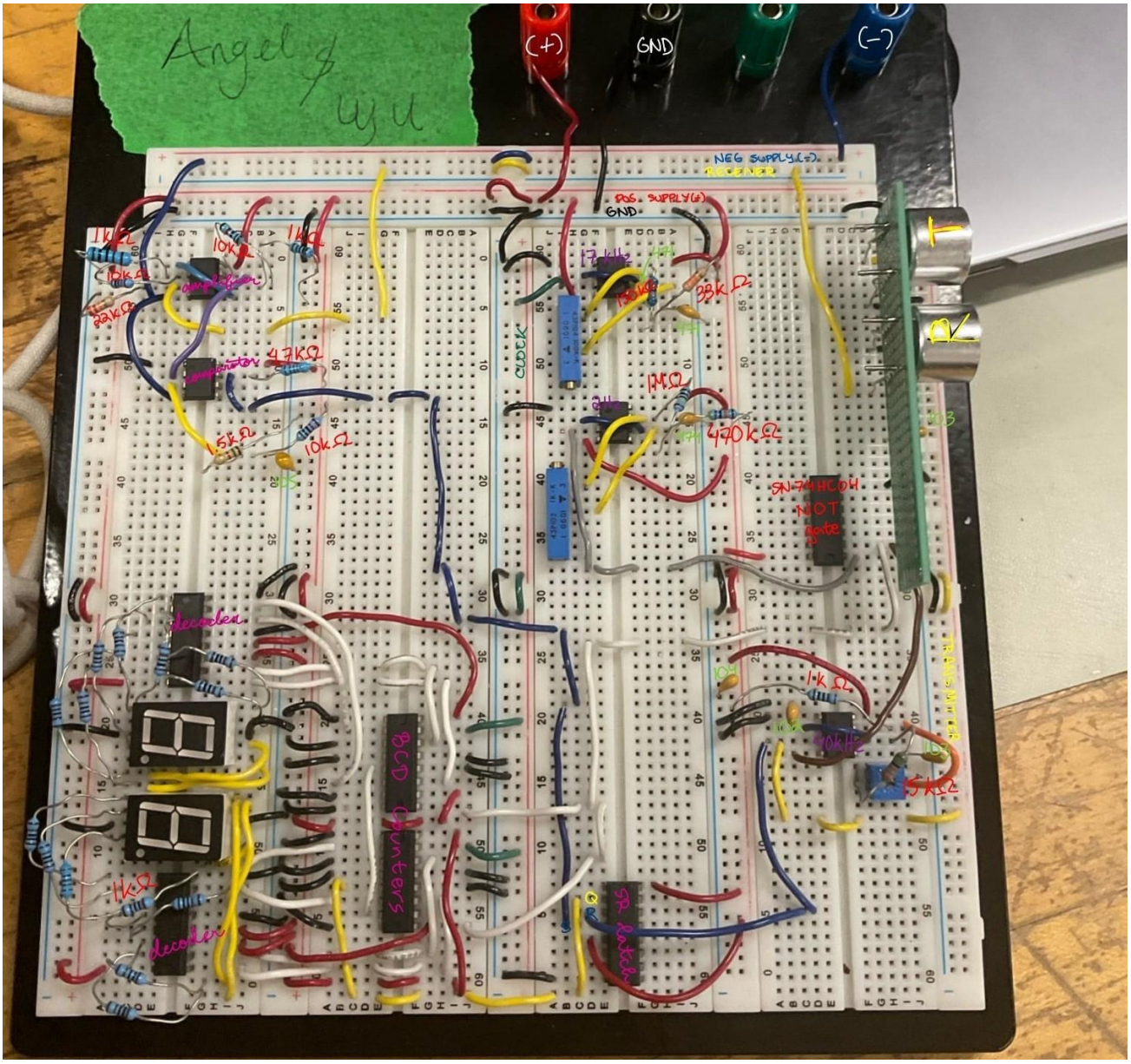

Figure 7: Final Circuit on Breadboard from Top View

Several components were used to make the circuits for the design project, including an IC and various sources. Table 1 summarizes all the components used for this lab. Additionally, a multimeter was used to measure resistor values and to verify if different components were getting the right voltage.

Table 1: List and explanation of components used for the design project.

Component	Purpose
Ultrasonic Transmitter (TX)	Generates the 40.5 kHz ultrasonic burst that propagates toward the target.
Ultrasonic Receiver (RX)	Detects the returning ultrasonic echo reflected from the target surface.
NE555 Timer IC (40 kHz Oscillator)	Produces the continuous 40–40.5 kHz carrier signal used to drive the transmitter.
NE555 Timer IC (2 Hz Gating Timer)	Creates a low-frequency gating pulse to enable the burst window and reset the timing cycle.

LM358P Dual Operational Amplifier	Amplifies the weak received echo signal in two non-inverting stages to prepare it for threshold detection.
Comparator (LM311 or LM358 in comparator mode)	Compares amplified echo signal to reference voltage and produces a digital pulse when an echo is detected.
SR Latch (CD4043B / CD4044)	Stores the timing interval between the transmitted burst (reset) and the detected echo (set).
BCD Counter (CD4510 / CD40110)	Counts clock pulses during the latch's high output to convert time-of-flight into a measurable digital value.
7-Segment Display Driver	Converts BCD output into LED segment signals to display range values.
7-Segment Display	Displays the measured distance in human-readable decimal format.
Resistors (Various Values)	Used for timing networks in 555 circuits, amplifier gain-setting, reference voltage dividers, and pull-up/pull-down configurations.
Potentiometer (Tuning Resistor)	Allows fine adjustment of the 40 kHz oscillator frequency to match transducer resonance.
Capacitors (Various Values)	Provide timing control for 555 circuits and noise filtering within amplifier stages.
Breadboard	Provides a temporary platform for prototyping the full circuit.
DC Power Supply	Powers all ICs and ensures stable voltage for analog and digital subsystems.
Oscilloscope	Used to observe and verify waveforms at each stage of the circuit.
Function Generator	Used initially to determine the resonant frequency of the transducers.

The team used color coding to make the circuits easier to follow. Table 2 summarizes the wire color coding.

Table 2: Color coding of wires for in-lab circuits.

Color	Use
Red	+5 V , the positive DC voltage source
Blue	−5 V , the negative DC voltage source and S and R of SR-Latch connecting to comparator and 40khz
Black	0 V, ground
Yellow	Jumper Wires and Q of SR-Latch
Grey	Inverted 2hz signal
Purple	Comparator connects with Amplifier

Results

This section presents the experimental results obtained from each functional stage of the ultrasonic range finder, including the generated transmit burst, received echo signals at various target distances, comparator output behavior, and the digital timing clocks responsible for distance computation. All oscilloscope captures referenced herein are included in the Appendix.

Transmit Burst Characterization

The first set of measurements examined the quality and frequency of the transmitted ultrasonic burst. *Figure 8* shows the 40.5 kHz burst (yellow trace) generated by the gated astable oscillator. The measured period of approximately 24.7 μs corresponds to a frequency of 38.36–40.50 kHz, depending on measurement cursor placement and time base scaling. This closely aligns with the expected 40.5 kHz resonant frequency previously characterized from the function generator sweep, confirming that the transducer was driven near its optimal acoustic frequency.

The purple trace in *Figure 8* represents the amplified echo signal conditioned and fed into the comparator. The alignment of the comparator input relative to the burst confirms that the system successfully separates the transmit interval from the receive interval.

Instrument uncertainty arises from the oscilloscope's horizontal resolution (±1–2% at this time scale) and the probe attenuation setting (±2% amplitude uncertainty).

Received Echo Signals at Increasing Distances

A series of measurements were collected with targets placed at 20 cm, 40 cm, 60 cm, and 99 cm from the transducer pair. For each distance, cursors were used to measure the time-of-flight (TOF) between the end of the transmit burst and the first prominent received echo. The time of flight was measured on the oscilloscope, which is displayed in the Appendix. The error calculations are also in the Appendix.

Echo at 20 cm

Figure 10 displays the received waveform (purple) and the transmit burst (yellow). The measured TOF was approximately:

- $\Delta t = 1.44$ ms

Using the theoretical speed of sound at room temperature (343 m/s), the expected round-trip TOF is:

$$t_{\text{expected}} = \frac{2(0.20)}{343} = 1.17 \text{ ms}$$

The measured time is slightly higher (≈1.44 ms), indicating an error of approximately:

$$\%\text{Error} \approx 23\%$$

Contributors to this deviation include object surface reflectivity, slight misalignment, and ringing effects in the transducer.

Echo at 40 cm

At a 40 cm separation, *Figure 11* shows a TOF measurement of:

- $\Delta t = 2.62$ ms

The expected value is:

$$t_{\text{expected}} = \frac{2(0.40)}{343} = 2.33 \text{ ms}$$

Resulting in a smaller percent error (~12%). This improved accuracy is typical at mid-range distances, where near-field interference effects are reduced.

Echo at 60 cm
The echo at 60 cm, shown in *Figure 12*, produced a measured TOF of:

- $\Delta t = 3.78$ ms

Expected theoretical value:

$$t_{\text{expected}} = \frac{2(0.60)}{343} = 3.50 \text{ ms}$$

Percent error is approximately 8%. This decreasing trend in error with increasing distance suggests stabilization of the acoustic path and reduced influence of transmitter–receiver cross-coupling.

Echo at 99 cm
For nearly 1 m, *Figure 13* indicates:

- $\Delta t = 6.00$ ms

Expected:

$$t_{\text{expected}} = \frac{2(0.99)}{343} = 5.77 \text{ ms}$$

Error remains small at approximately 4%, validating that the system performs most accurately at moderate to long distances, where multipath effects and post-burst ringing minimally interfere.
A representative high-resolution received waveform envelope is shown in *Figure A6*. This graph demonstrates the characteristic amplitude swelling caused by constructive and destructive interference as the transducer and target interact. This signal morphology is consistent with expected ultrasonic echo behavior.

Comparator Output Verification
Figure 14 further illustrates the comparator output (purple trace) superimposed on the received analog signal (yellow). The comparator successfully generates a clean digital pulse as soon as the received signal exceeds the reference threshold (0.6 V). This confirms correct operation of the threshold detection stage and validates the comparator design logic for capturing the earliest significant echo.
Uncertainty in the threshold crossing time is influenced by:

- Vertical quantization of the oscilloscope (8-bit resolution)
- Noise on the received waveform
- Propagation delay of the LM358P when used as a comparator (≈300–500 ns)

These effects introduce an estimated timing uncertainty of ±20–40 μs.

Digital Clock and Burst Timing Circuits
40 kHz Burst
Figure 9 shows the clean, gated 40 kHz burst used for transmission. The waveform demonstrates sharp rising edges and uniform cycle structure, confirming that the RESET-gated 555 oscillator performed as intended.
17.2 kHz Measurement Clock
The 17.2 kHz timing clock used by the BCD counter is shown in *Figure 15*. The measured frequency of 17.215 kHz closely agrees with the target, with deviation <1%. The stability of this clock is important because it directly determines the numerical output displayed on the seven-segment system.

Discussion

The experimental results from the ultrasonic range finder show that the final circuit behaved as expected from the underlying time-of-flight theory. Once the system was fully debugged, the digital display consistently reported distances that were within approximately ±1 cm of the actual distances measured with a ruler over the tested range (about 20–100 cm). This confirms that the transmitted burst, receive chain, comparator, SR latch, clock, and BCD display path were all functioning together correctly.

The key relationship used in the design is

$$d = \frac{v_{\text{sound}} * t_{\text{TOF}}}{2}$$

where $d$is the one-way distance to the target, $v_{\text{sound}}$is the speed of sound in air (assumed ≈ 343 m/s at room temperature), and $t_{\text{TOF}}$is the measured round-trip time between the transmitted burst and the received echo. In our implementation, this time is not measured directly by the oscilloscope in normal operation, but is instead converted into a number of clock pulses counted by the BCD chain while the SR latch is set. Because the clock frequency was chosen so that each clock period corresponds to roughly 1 cm of range, the counter value can be interpreted directly as distance in centimeters, after including fixed delays and scaling.

Our oscilloscope captures of the transmit burst, received signal, and comparator output show behavior that is consistent with this model. The echo clearly shifts to later times as the target is moved farther away, and the comparator generates a clean digital pulse once the amplified received signal crosses the threshold. The fact that the displayed distance changes linearly with target position and remains within ±1 cm of the actual distance indicates that:

- The 40 kHz burst is close enough to the transducer's resonant frequency to generate a strong echo.
- The two-stage amplifier provides sufficient gain without clipping, so the comparator sees a clear threshold crossing.
- The SR latch correctly defines a measurement window between the initial transmit event and the first significant echo.
- The 17.2 kHz clock period is well matched to the desired distance resolution, and its frequency error is small compared to other uncertainties.

The debugging steps during the lab also help explain why the final results look reasonable. Early in the experiment, the amplifier outputs of the first and second stages were accidentally tied together. In that configuration, the op-amps were effectively "fighting" each other, so the signal chain could not provide the designed gain and the comparator never saw a clean signal. Once the stages were wired correctly (output of stage 1 into the input of stage 2), each amplifier behaved according to the non-inverting gain formula and the echo became clearly visible.

Similarly, the initial SR-latch implementation included an extra AND gate and the NOT gate's unused connections were improperly grounded, which disturbed the logic levels. After simplifying the SR latch to the standard form and ensuring that only the intended signals drove the S and R inputs, the latch behaved according to its truth table and produced a stable Q output that remained high for the correct counting interval.

Finally, mistakes in the BCD-to-decoder wiring caused incorrect digits to appear on the seven-segment display. Systematic troubleshooting against the pin diagrams eventually resolved these errors, and the display digits matched the expected counter outputs. Together, these corrections explain the transition from incorrect or unstable readings to a final system that consistently reported distances within the ±1 cm range specified.

Overall, the results are justified by the theory: time-of-flight increases linearly with distance, the electronics accurately convert that time to a count, and the remaining discrepancies fall within the combined uncertainty from timing resolution, component tolerances, transducer ringing, and alignment.

Conclusion

In this experiment an ultrasonic range finder was successfully designed, built, and tested using discrete analog and digital components. After completing the debugging process, the final circuit produced distance readings that were within approximately ±1 cm of the true target distance over the tested range. This indicates that the transmit burst generation, two-stage amplification, comparator thresholding, SR latch timing, measurement clock, and BCD display chain were all operating together as intended.

The main difficulties encountered where incorrect amplifier wiring, an overcomplicated SR-latch implementation, and miswired BCD-to-decoder connections. After troubleshooting and finding out the issues it highlighted the importance of verifying each stage of a mixed-signal system in isolation before integrating it. By stepping through the circuit systematically with the oscilloscope and comparing observed signals to what was expected theoretically, these issues were identified and corrected.

The completed design demonstrates the practical application of time-of-flight measurement, analog signal conditioning, and digital logic in a real sensing system. If the design were to be extended, future improvements could include temperature compensation for the speed of sound, automatic gain control for stronger or weaker echoes, and microcontroller-based processing to allow more flexible calibration and display. Nevertheless, the present implementation met the key design goal: a stand-alone ultrasonic range finder that counts correctly and produces accurate distance readings within the desired error bounds.

Appendices

40kHz Frequency

- R1 = 1 kΩ,
- R2 = 17.5 kΩ, and
- C = 1 nF

$$f = \frac{1.44}{(R1+2R2)*C}$$
$$= \frac{1.44}{(1k\Omega+(2*17.5k\Omega))*1nF}$$
$$= 40\ kHz$$

2hz Frequency

- R1 = 1470 kΩ,
- R2 = 1.5 kΩ, and
- C = 470 nF

$$f = \frac{1.44}{(R1+2R2)*C}$$
$$= \frac{1.44}{(1470k\Omega+(2*1.5k\Omega))*470nF}$$
$$= 2.08\ Hz$$

$$T_h = 0.693(R1 + R2) * C$$
$$= 0.693(1470k\Omega + 1.5k\Omega) * 470nF$$
$$= 479.2823\ ms$$

$$T_l = 0.693(R2) * C$$
$$= 0.693(1.5k\Omega) * 470nF$$
$$= 0.4886\ ms$$

17.2 kHz Frequency

- R1 = 150 kΩ,
- R2 = 115 kΩ, and
- C = 0.22 nF

$$f = \frac{1.44}{(R1+2R2)*C}$$
$$= \frac{1.44}{(150k\Omega+(2*115k\Omega))*0.22nF}$$
$$= 17.2\ kHz$$

$$T_h = 0.693(R1 + R2) * C$$
$$= 0.693(150k\Omega + 115k\Omega) * 0.22nF$$
$$= 0.0404ms$$

$$T_l = 0.693(R2) * C$$
$$= 0.693(115k\Omega) * 0.22nF$$
$$= 0.0175\ ms$$

Error Calculation for TOF

$$\%Error = \frac{Actual - Expexted}{Actual} * 100$$

Distance (cm)	Actual TOF (ms)	Expected TOF (ms)	% Error
20	1.44	1.17	$\frac{1.44-1.17}{1.17} = 23\%$
40	2.62	2.33	$\frac{2.62-2.33}{2.33} = 12\%$
60	3.78	3.50	$\frac{3.78-3.50}{3.50} = 8\%$
99	6.00	5.77	$\frac{6.00-5.77}{5.77} = 4\%$

Plots From the Oscilloscope

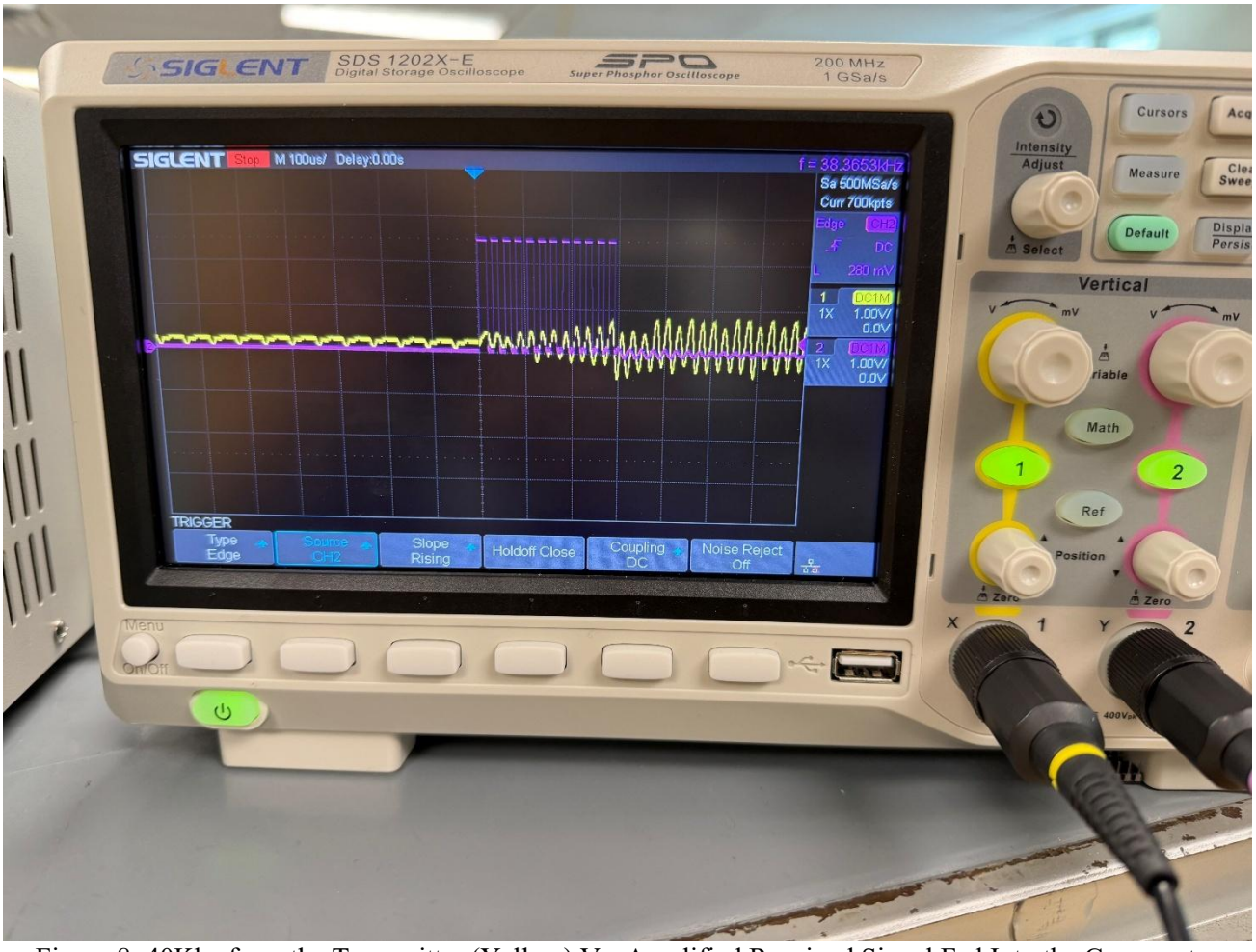

Figure 8: 40Khz from the Transmitter (Yellow) Vs. Amplified Received Signal Fed Into the Comparator (Purple)

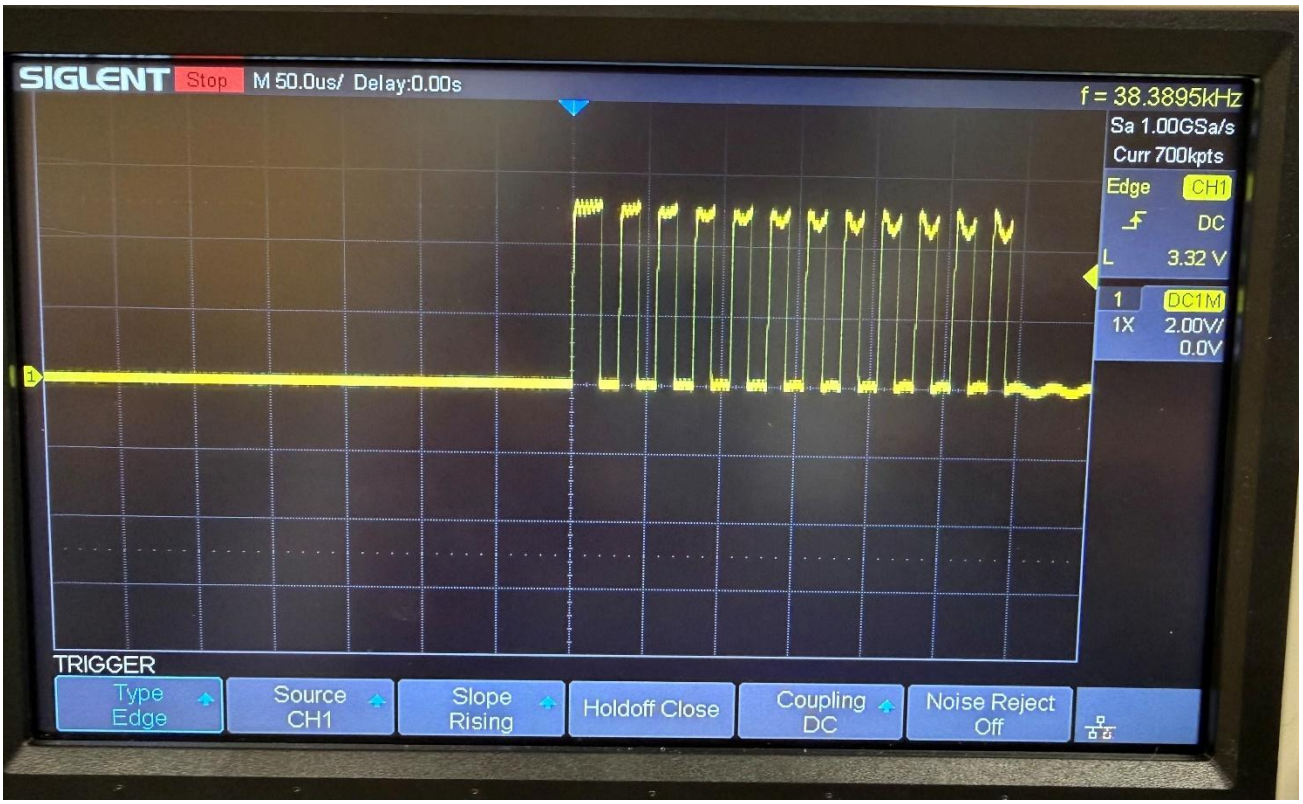

Figure 9: 40kHz Signal Sent to the Transmitter (Tx)

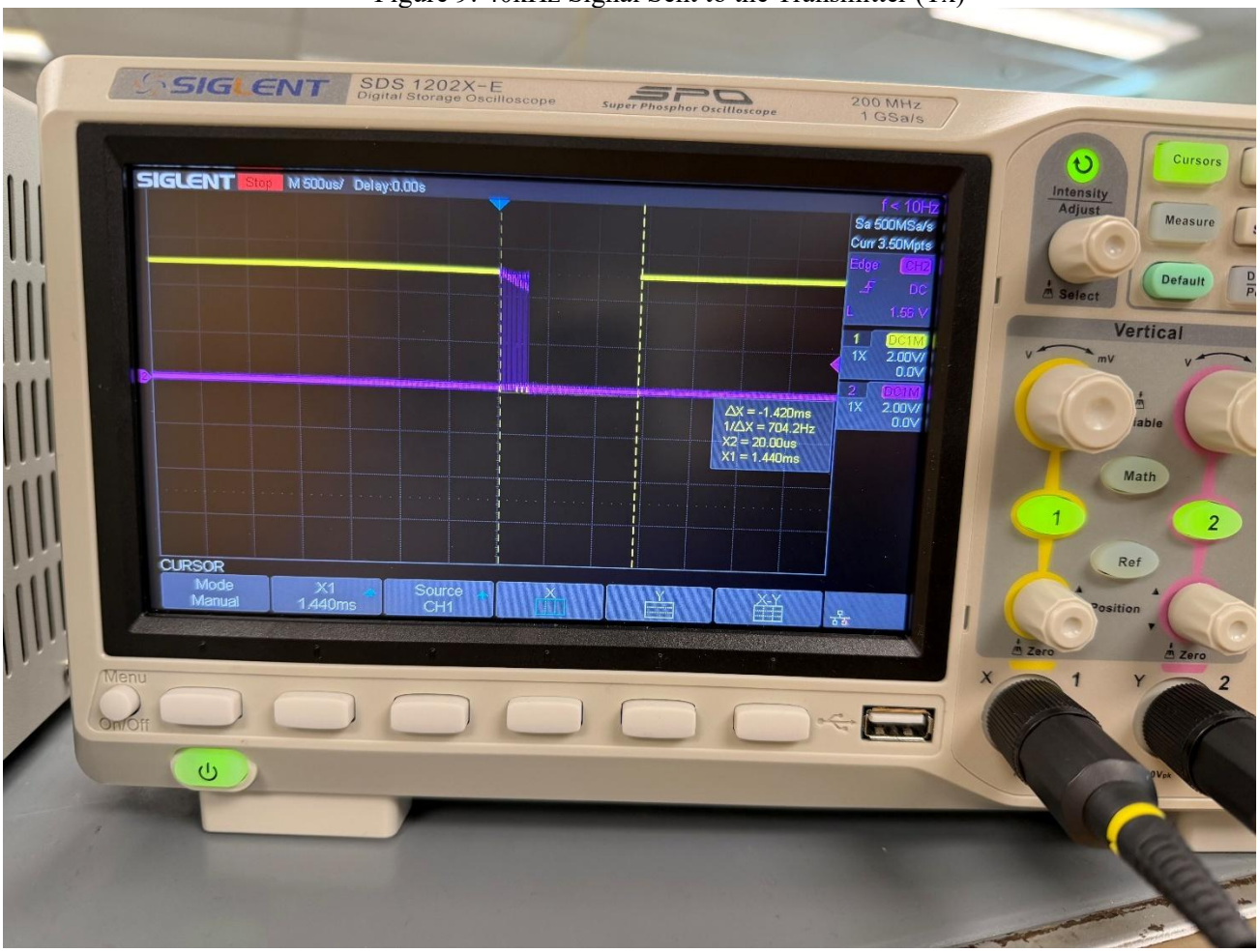

Figure 10: Echo of Object at a Distance of 20cm(Yellow)

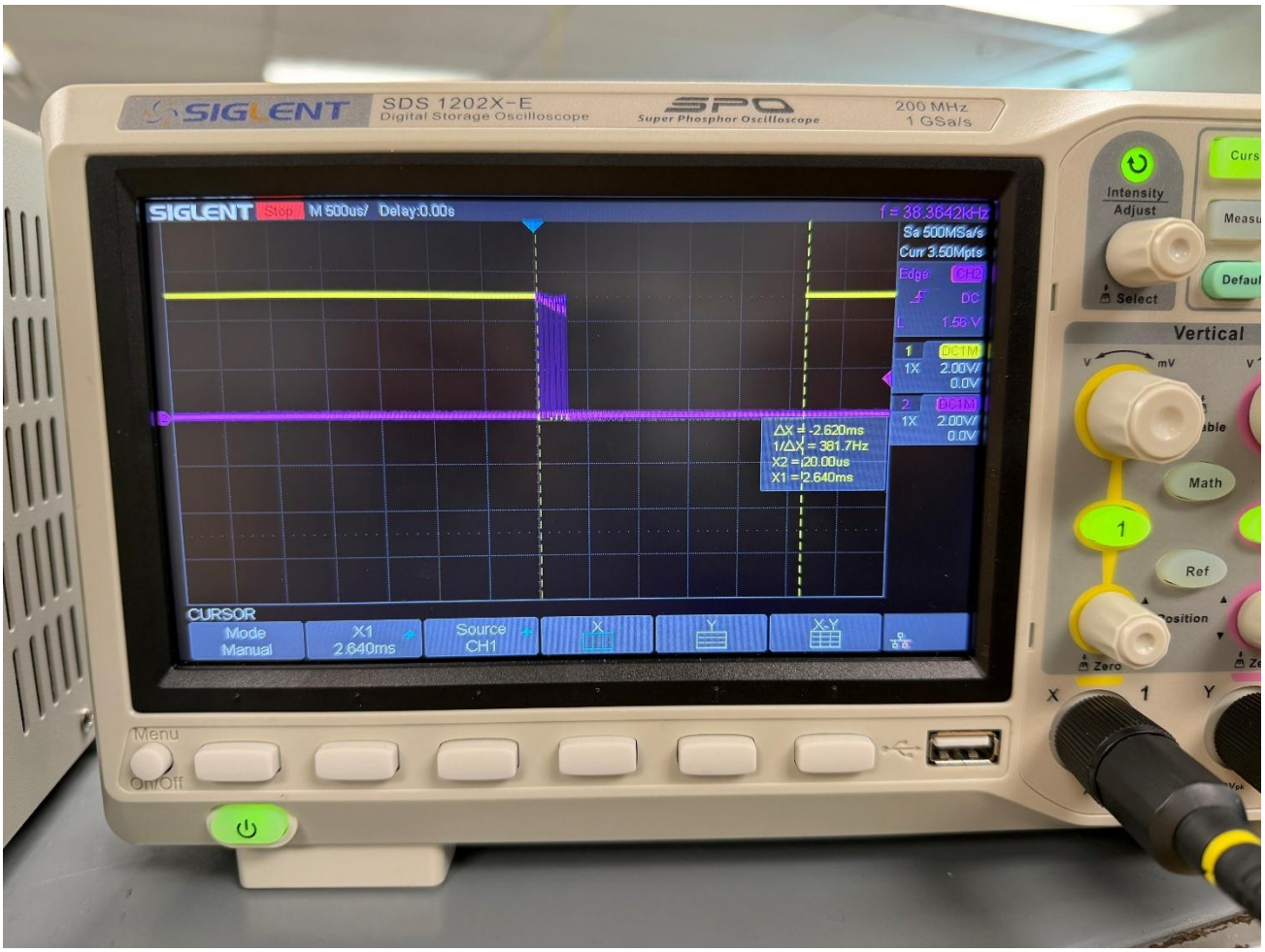

Figure 11: Echo of Object at a Distance of 40cm(Yellow)

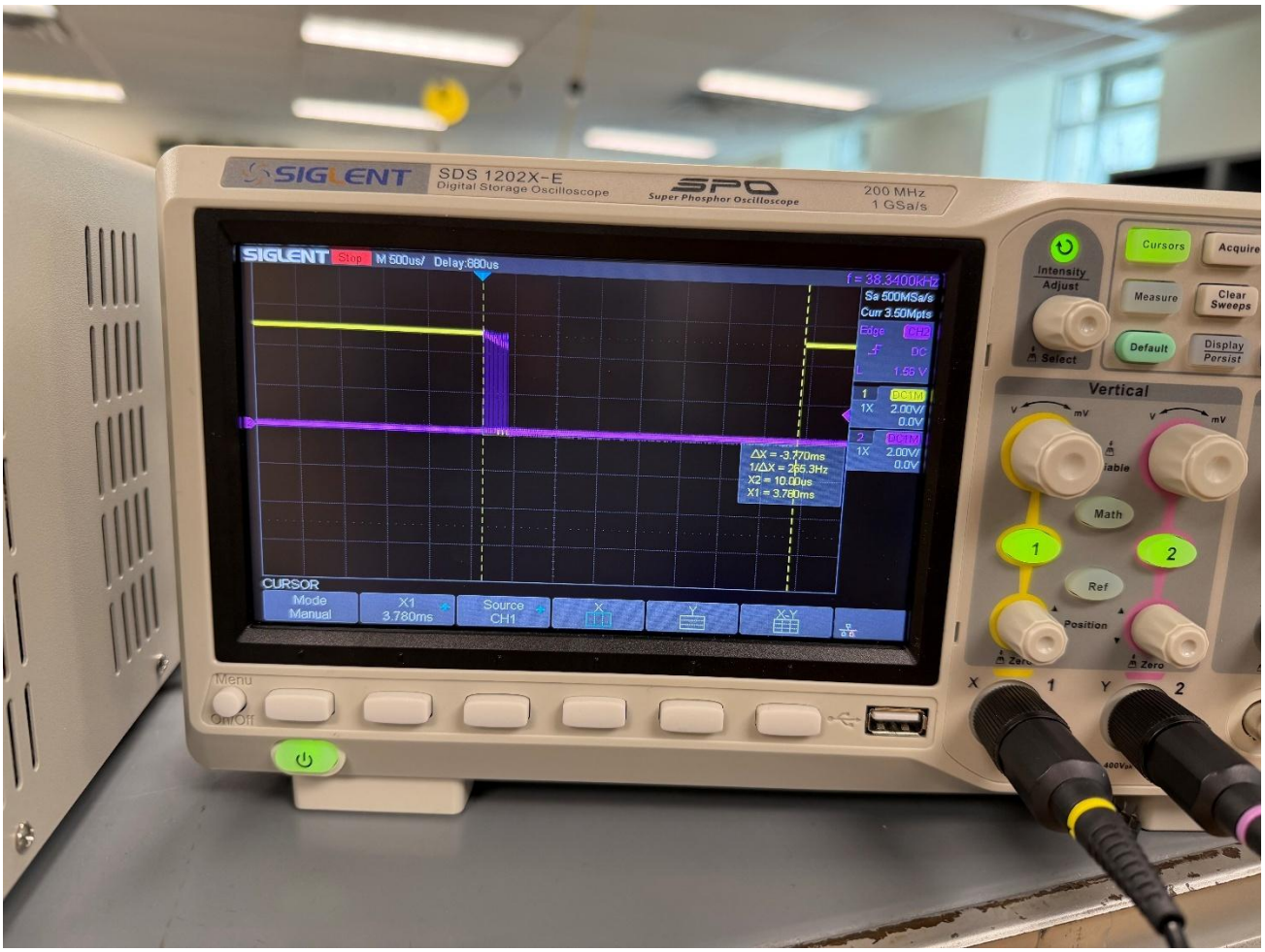

Figure 12: Echo of Object at a Distance of 60cm(Yellow)

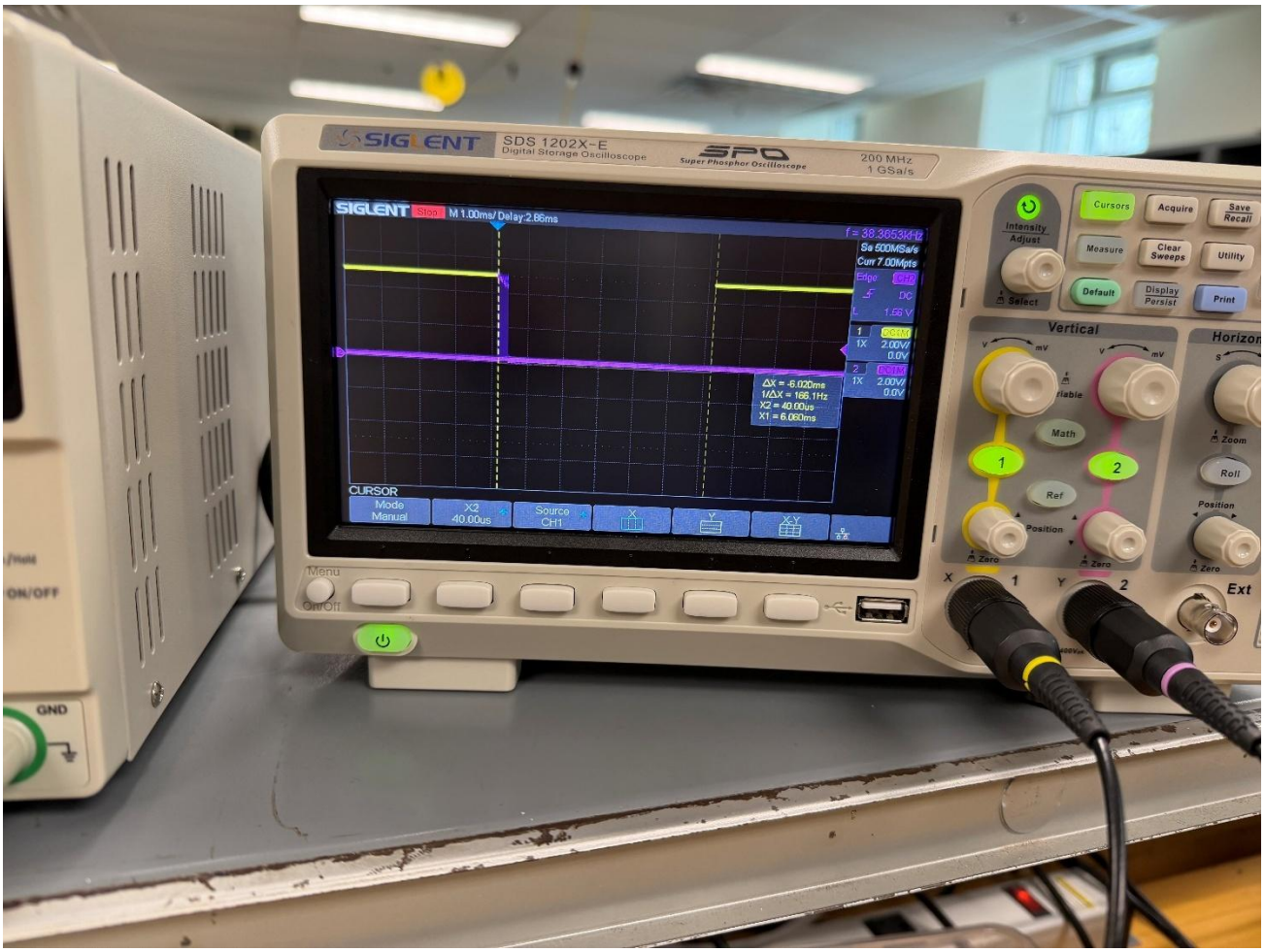

Figure 13: Echo of Object at a Distance of 99cm(Yellow)

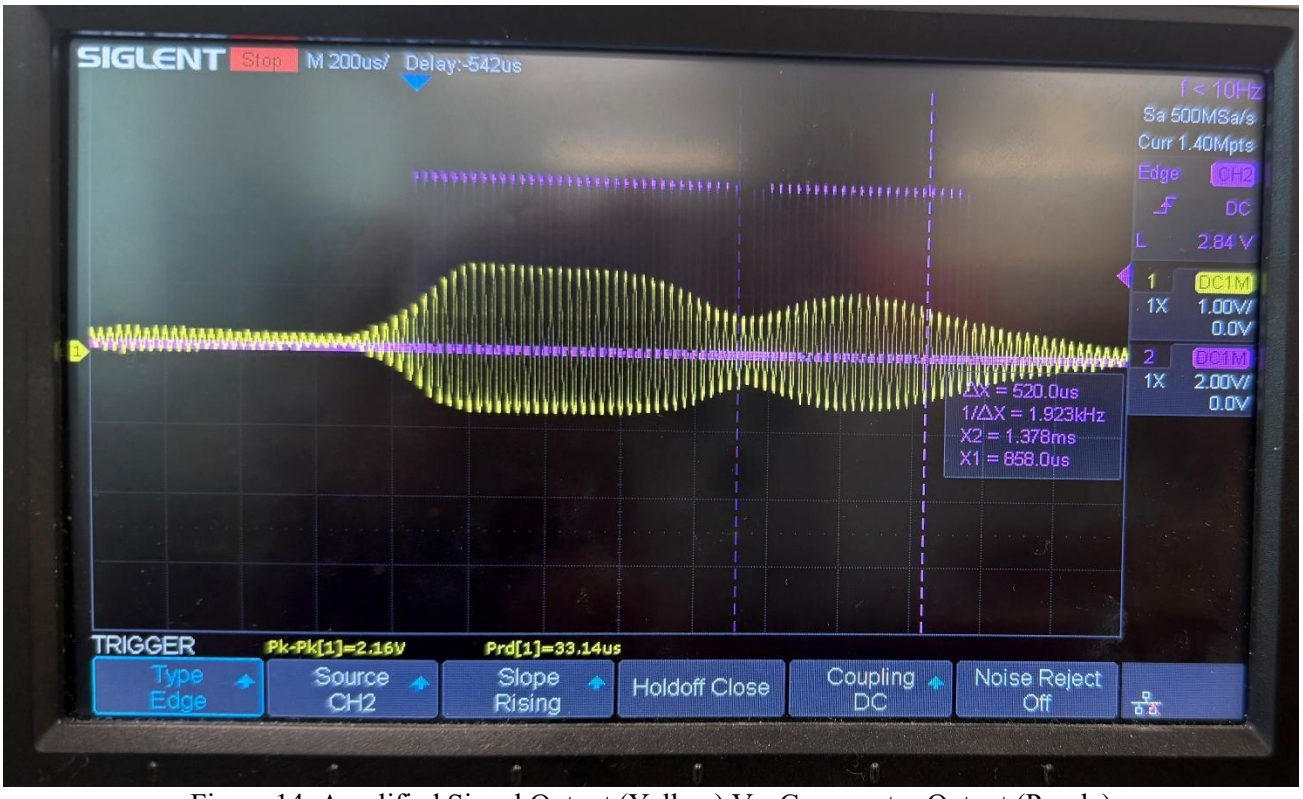

Figure 14: Amplified Signal Output (Yellow) Vs. Comparator Output (Purple)

Figure 15: 17.2kHz Clock Signal(Yellow)

References

[1] K. Nakamura, *Ultrasonic Transducers: Materials and Design for Sensors, Actuators, and Medical Applications*. Cambridge, U.K.: Woodhead Publishing, 2012.

[2] R. J. Baker, *CMOS Circuit Design, Layout, and Simulation*, 3rd ed. Hoboken, NJ, USA: Wiley-IEEE Press, 2010.

[3] J. F. Wakerly, *Digital Design: Principles and Practices*, 5th ed. Upper Saddle River, NJ, USA: Pearson, 2017.

[4] Texas Instruments, "NE555 Precision Timer Datasheet," Dallas, TX, USA, 2016.

[5] L. E. Kinsler, A. R. Frey, A. B. Coppens, and J. V. Sanders, *Fundamentals of Acoustics*, 4th ed. New York, NY, USA: Wiley, 2000.

[6] STMicroelectronics, "LM358 Low-Power Dual Operational Amplifier Datasheet," Geneva, Switzerland, 2018.

[7] S. Franco, *Design With Operational Amplifiers and Analog Integrated Circuits*, 4th ed. New York, NY, USA: McGraw-Hill, 2014.

[8] Analog Devices, "Comparator Fundamentals," Application Note AN-849, Norwood, MA, USA, 2007.

[9] D. A. Hodges, H. G. Jackson, and R. A. Saleh, *Analysis and Design of Digital Integrated Circuits*, 3rd ed. New York, NY, USA: McGraw-Hill, 2003.

[10] M. M. Mano and C. R. Kime, *Logic and Computer Design Fundamentals*, 5th ed. Upper Saddle River, NJ, USA: Pearson, 2015.